AD-A054 962 NAVAL COASTAL SYSTEMS CENTER PANAMA CITY FL F/G 13/10.1
HYDRODYNAMIC STABILITY AND CONTROL ANALYSIS OF 6TOPS VEHICLE.(U)
MAY 78 D C SUMMEY, N S SMITH, K W WATKINSON

UNCLASSIFIED NCSC-TR-323-78 NL

1 OF 1
AD
A054 962

END
DATE
FILMED
7-78
DDC

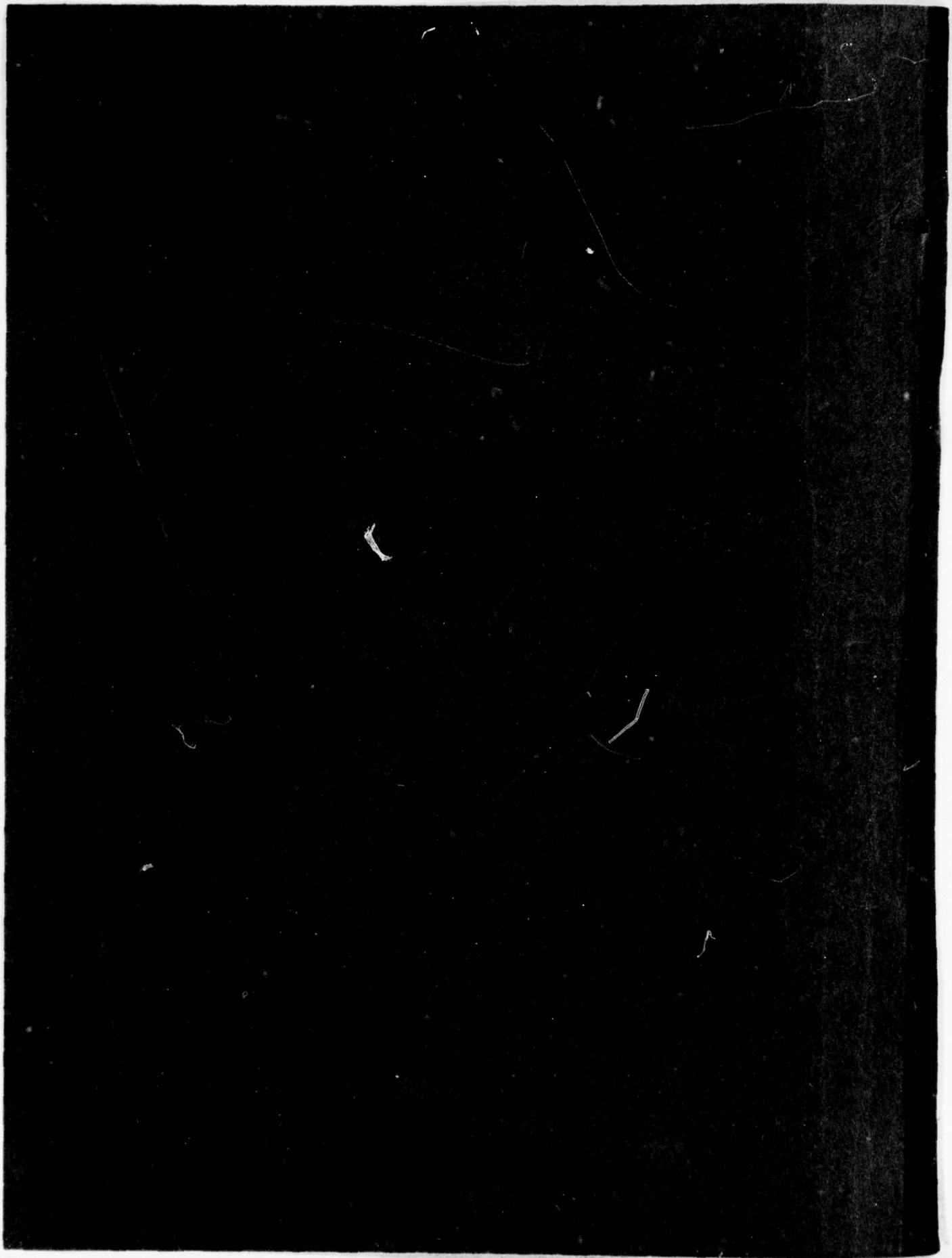

UNCLASSIFIED

SECURITY CLASSIFICATION OF THIS PAGE (When Data Entered)

REPORT DOCUMENTATION PAGE

READ INSTRUCTIONS BEFORE COMPLETING FORM

1. REPORT NUMBER: NCSC-TR-323-78
2. GOVT ACCESSION NO.:
3. RECIPIENT'S CATALOG NUMBER:
4. TITLE (and Subtitle): HYDRODYNAMIC STABILITY AND CONTROL ANALYSIS OF GTOPS VEHICLE
5. TYPE OF REPORT & PERIOD COVERED: Technical Report
6. PERFORMING ORG. REPORT NUMBER:
7. AUTHOR(s): D. C. Summey, N. S. Smith, K. W. Watkinson and D. E. Humphreys
8. CONTRACT OR GRANT NUMBER(s):
9. PERFORMING ORGANIZATION NAME AND ADDRESS: Naval Coastal Systems Center, Panama City, Florida 32407
10. PROGRAM ELEMENT, PROJECT, TASK AREA & WORK UNIT NUMBERS:
11. CONTROLLING OFFICE NAME AND ADDRESS:
12. REPORT DATE: May 1978
13. NUMBER OF PAGES: 37 (12 40 p.)
14. MONITORING AGENCY NAME & ADDRESS (if different from Controlling Office):
15. SECURITY CLASS. (of this report): UNCLASSIFIED
15a. DECLASSIFICATION/DOWNGRADING SCHEDULE: N/A

16. DISTRIBUTION STATEMENT (of this Report)

Approved for public release. Distribution unlimited.

17. DISTRIBUTION STATEMENT (of the abstract entered in Block 20, if different from Report)

(cont'd p. 1)

18. SUPPLEMENTARY NOTES

Geometric variations of the

19. KEY WORDS (Continue on reverse side if necessary and identify by block number)

Underwater vehicles
Hydrodynamics
Stability
Dynamic response
Design
Control

Identifiers:
Hydrodynamic stability
Towed underwater vehicle
GTOPS
Twin hull vehicle
Mass distribution

20. ABSTRACT (Continue on reverse side if necessary and identify by block number)

A twin-hulled hydrodynamic (GTOPS) vehicle has been designed and analyzed, based on certain geometric and operational constraints. From a conceptual sketch of the body, base case towed vehicle geometry was defined, and geometry variations were conducted to optimize vehicle stability and trajectory performance. The geometric variations which were investigated included: the effects of wing position, horizontal and vertical tail size and shape, vehicle center of gravity and center of buoyancy separation, body-body

(over)

DD FORM 1 JAN 73 1473 / EDITION OF 1 NOV 65 IS OBSOLETE

S/N 0102-LF-014-6601

410650

SECURITY CLASSIFICATION OF THIS PAGE (When Data Entered)

19.

Root locus
Tethering

20. (cont)

separation distance, body shape, and speed variations from 2 to 12 knots. Root locus diagrams are presented for selected geometric variations, and time history trajectories are included for various tether tensions and control surface inputs.

TABLE OF CONTENTS

LIST OF ILLUSTRATIONS

LIST OF TABLES

(Reverse Page iv Blank)

INTRODUCTION

In response to a request from Applied Physics Laboratory at Johns Hopkins University for a dynamic analysis of an underwater vehicle design, NCSL conducted an investigation of the Gibson's Towed Profiling System (GTOPS) vehicle.

The vehicle consisted of two like bodies joined by a wing and tail appendages. The configuration of the bodies was set, but the size and configuration of the appendages were subject to change. The vehicle was sized and analyzed to determine longitudinal and lateral stability.

The analysis included the effects of geometric changes, tow cable considerations, twin fuselage interference drag, the effects of depth-keeping tethers, horizontal tail actuator sizing, and time domain dynamic vehicle response. Each of these considerations is discussed.

(cont on p 14 73A)

VEHICLE CONFIGURATION

CONFIGURATION CONTROL

The external configuration of the GTOPS vehicle had been controlled primarily by the following factors:

1. Payload Characteristics. Each body would house an axisymmetric instrumentation device. The two bodies are joined by a wing allowing enough separation distance to avoid interference between the instrumentation.

2. Variable Depth/Towed Operation Requirement. The vehicle must have the capability to change or hold towing depth via remote control.

3. Dynamic Stability. Due to the nature of the measurements to be taken, high damping ratios and low modal frequencies were desirable vehicle characteristics.

4. Drag Minimization. In order to permit smooth operation of the roller/cable assembly, the vehicle must not distort the cable catenary in the region of the towpoint.

Factors 1 and 4 led to the twin hull GTOPS configuration using a streamlined form[1]. Two nearly identical body forms were chosen for analysis. Both forms were dependent upon the size and shape of the instrumentation packages to be housed in the bodies. The geometric characteristics of the two forms were:

Position of Maximum Cross-Section X_m	Nose Radius R_n	Tail Radius R_t	Prismatic Coefficient C_p	Fineness Ratio L/D	
0.36	0.7	0.3	0.65	6.55	- 655 Body
0.36	1.0	0.3	0.65	7.51	- 751 Body

The 655 hull shape was chosen for the baseline body configuration in the interest of reducing size and weight.

FORWARD WING

The envelope of the hardware to be housed inside of the forward wing led to the selection of an 0021 airfoil section shape with a chord length of 1.5 feet. The distance between the bodies (root chord to root chord at maximum body cross-sectional area) was 2.0 feet, giving a body centerline separation of 2.92 feet. This distance was chosen with regard to the lifting force required of the forward surface for depth change response.

ELEVATOR

The elevator design was dependent upon:

1. control effectiveness required,
2. longitudinal stability, and
3. hinge moment/actuator sizing.

The basic design criteria was to keep the size of the elevator as small as possible while still providing adequate effectiveness and stability. This criteria was intended to minimize hinge moments and vehicle unsteadiness due to actuator slop. An all moveable elevator design with a chord of 0.5 feet and a section shape of an 0020 airfoil was selected. Shape and size of the vertical fins were almost entirely dependent upon stability considerations.

---

[1] David Taylor Model Basin Report 719 *Mathematical Formulations of Bodies of Revolution*, by L. Landweber and M. Gertler, September 1950.

FINAL VEHICLE DESIGN

The foregoing brief discussion of the GTOPS vehicle gives a general idea of the design criteria used. The variational analyses provide further design information. The resulting vehicle design is shown in Figures 1, 2, and 3. The mass distribution data are given in Table 1.

TABLE 1

MASS DISTRIBUTION DATA

Vehicle displaced weight (lb)	373.0
Vehicle displaced volume (ft^3)	5.82
Body wetted area (ft^2)	26.92
Longitudinal location of c.g. (ft) (from nose)	2.66
Longitudinal location of c.b. (ft) (from nose)	2.66
Vertical distance c.b. to c.g (ft) (positive down)	0.0417
X-axis inertia moment (slug-ft^2)	9.0328
Y-axis inertia moment (slug-ft^2)	7.4910
Z-axis inertia moment (slug-ft^2)	16.189

GEOMETRIC VARIATIONS AND STABILITY ANALYSIS

In order to determine the effectiveness of the base case design, several computer analyses were made on the GTOPS vehicle with variations from the base case. By analyzing the stability of these modified vehicles a sensitivity analysis of the base case geometry was obtained. Table 2 describes both the type and magnitude of base case variations considered.

(Text Continued on Page 7)

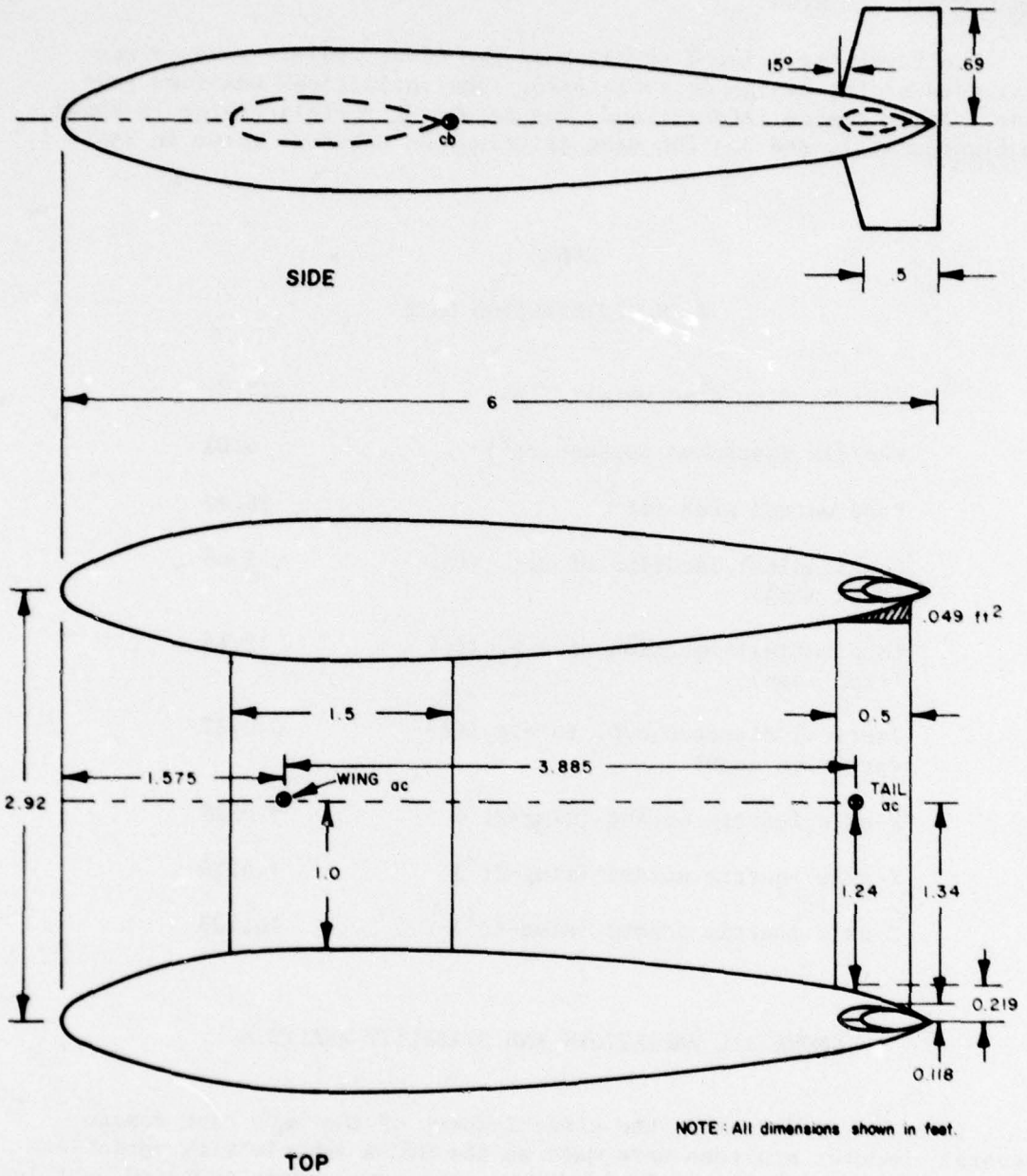

FIGURE 1. GTOPS TWIN-FUSELAGE VEHICLE 655

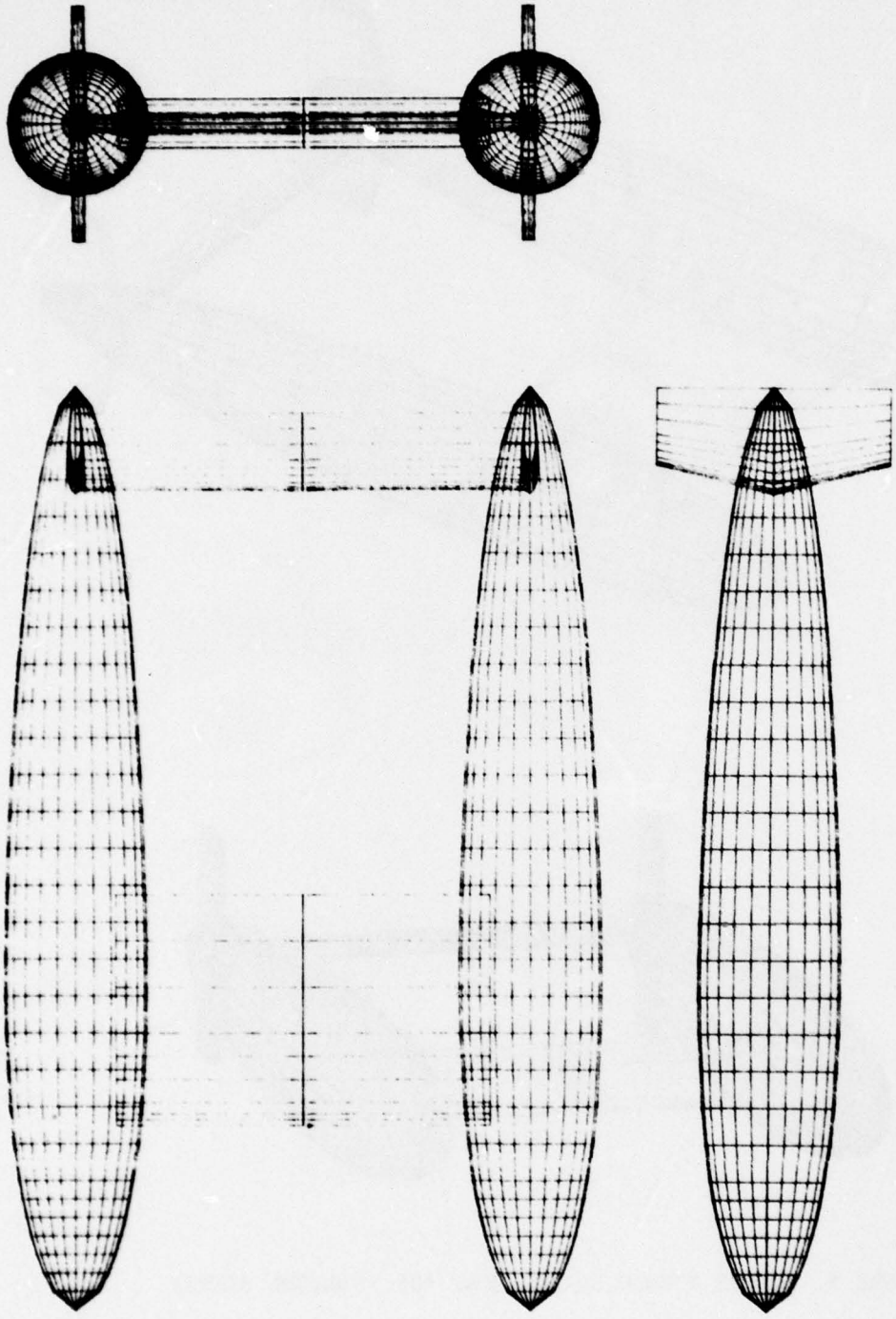

FIGURE 2. GTOPS DOUBLE HULLED BODY 655 (TOP, SIDE, AND FRONT VIEWS)

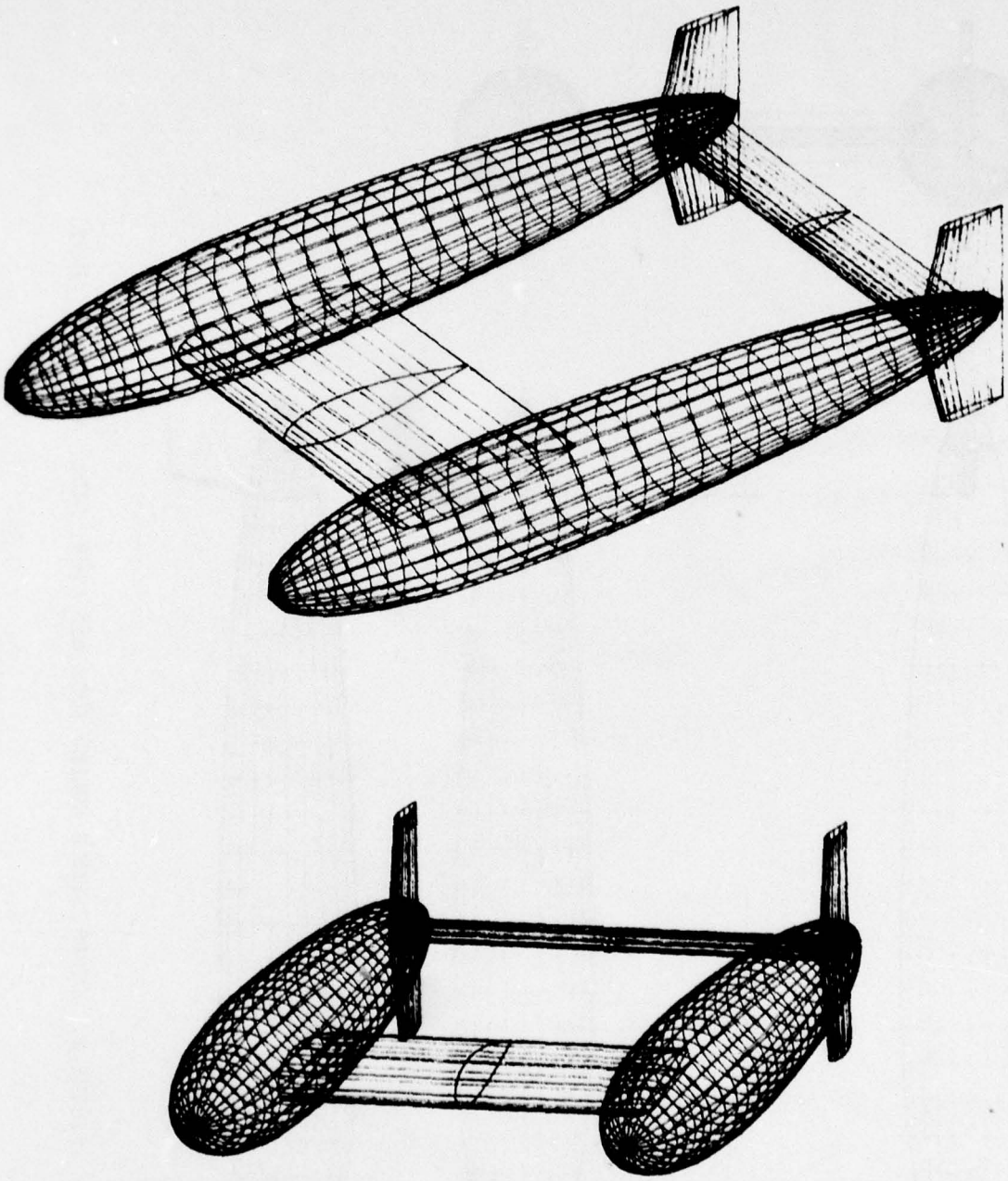

FIGURE 3. GTOPS DOUBLE HULLED BODY 655 (OBLIQUE VIEWS)

TABLE 2

VEHICLE BASE CASE VARIATIONS FOR ANALYSIS

Data File Number	Geometry Variation	Magnitude
1	Base Case Geometry	
2	Distance between nose and ac	1.0'
3	of wing (base case = 1.575')	2.75' (at cb location)
4	Aspect ratio of tail by varying	9" chord
5	horizontal tail chord (base case = 6",	3" chord
6	Vertical cb-cg separation	cg ½" above cb
7	(base case had no separation)	cg ½" below cg
8	Body-body separation distance	1' span
9	(base case = 2' wing span)	3' span
10	X-position of vehicle cg	2" forward movement
11	(base case = 2.66' from nose)	2" aftward movement
12	Variation in weight and buoyancy	weight 20% > buoyancy
13	(base case is neutrally buoyant)	weight 20% < buoyancy
14	Vertical tail size	50% of original area
15	(base case = 0.355 ft^2)	150% of original area
16	Speed Variations	2 knots
17	(base case = 4 knots)	6 knots
18		8 knots
19		10 knots
20		12 knots
21	Body Shape (base case is 655 body)	New body is 751 body

STABILITY ANALYSIS

The basic stability of the various geometric configurations was determined using root locus techniques. By considering the locations of the roots of the characteristic equation of both the longitudinal and lateral transfer functions, basic system stability can be determined. A stable system must have all roots in the left-half plane (this corresponds to

roots with negative real parts). Both the longitudinal and lateral roots for each of the geometric variations are given in Table 3. Denominator and numerator roots for each of the longitudinal and lateral transfer functions are presented with gain values in Tables 4 and 5. The stability of the base case is considered along with a discussion of the effects of geometric variations.

BASE CASE

The base case vehicle proved to be stable in the longitudinal domain and neutrally stable in the lateral domain. The longitudinal roots were all real indicating that no oscillatory modes of motion were present (the base considered a cable but no tethers). The existence of only periodic roots means that when the vehicle is disturbed longitudinally it will return to equilibrium without overshoot or oscillatory motion. The lateral motion was also non-oscillatory and stable for all modes except roll where it was only neutrally stable due to a lateral root of zero (See Table 5). The lateral roll root at the root locus origin indicated that there is no mechanism to return the vehicle to a zero roll angle when a lateral disturbance is encountered due to the zero cb-cg separation. Sketches of both the pitch and yaw root loci are shown in Figures 4 and 5 for various cb-cg separations.

VARIATIONS

Figure 4 shows the root locus plot of the pitch transfer function for changes in cb-cg separation. Three cb-cg locations were analyzed, cg ½" below the cb, cg at the cb, and cg ½" above the cb. The pitch transfer function consists of four poles and two zeros[2][3]. Three of the poles and two of the zeros are not affected by cb-cg position. The one pole that does change is the characteristic mode of the system (i.e. the pole closest to the origin); therefore, the cb-cg position directly affects the response time of the vehicle. For the cg ½" below the cb this pole is located at (s + 0.057), yielding a settling time in pitch of $t_{0.95}$ = 115 seconds. Locating the cg ½" above the cb moves the pole into the right-hand plane to (s - 0.0045), yielding an unstable vehicle. It should be noted that when one compares the time histories presented later in the report with the settling time of 115 seconds, there appears to be a discrepancy; the time histories show very rapid response to pulse and doublet

---

[2] Naval Coastal Systems Laboratory Report 287-76, *Development of the Equations of Motion and Transfer Functions for Underwater Vehicles*, by D. E. Humphreys, July 1976.

[3] Naval Coastal Systems Laboratory Report 242-76, *The Analysis of a Longitudinal Control System for Underwater Vehicles*, by D. E. Humphreys, R. W. Miller and L. F. Dewberry, October 1975.

TABLE 3

LONGITUDINAL AND LATERAL ROOTS FOR GTOPS GEOMETRIC VARIATIONS

Geometry Variation	Data File #	Longitudinal Roots	Lateral Roots
Base Case	1	-0.026 -0.255 -4.23 -11.49	0.0 -0.086 -0.089 -1.38 -5.91
Distance Between Nose And Wing A.C.	2	-0.27 -0.26 -4.31 -11.49	0.0 -0.089 -0.108 -1.38 -5.90
	3	-0.21 -0.255 -3.43 -11.94	0.0 -0.047 -0.089 -1.39 -5.94
Aspect Ratio Of Tail	4	-0.028 -0.266 -4.31 -11.94	0.0 -0.090 -0.104 -1.38 -5.91
	5	-0.022 -0.243 -3.74 -8.20	0.0 -0.036 -0.082 -1.38 -5.91
C.B.-C.G. Separation	6	-0.0045 -0.255 -4.23 -11.51	0.0 -0.086 +0.323 -1.39 -5.91
	7	-0.57 -0.255 -4.23 -11.46	-0.087 -0.044 -j 0.362 -0.044 +j 0.362 -1.42 -5.92
Body-Body Separation	8	-0.037 -0.216 -2.33 -7.81	0.0 -0.019 -0.073 -1.41 -7.84
	9	-0.020 -0.293 -5.86 -14.42	0.0 -0.101 -0.268 -1.32 -4.28
X-C.G. Position	10	-0.025 -2.55 -4.000 -12.82	0.0 -0.080 -0.089 -1.30 -6.61
	11	-0.027 -0.255 -4.39 -10.26	0.0 -0.089 -0.094 -1.47 -5.22
Weight And Buoyancy	12	-0.026 -0.214 -3.97 -11.37	0.0 -0.80 -0.89 -1.38 -5.81
	13	-0.026 -0.315 -4.53 -11.64	0.0 -0.089 -0.093 -1.39 -6.05
Vertical Tail Size	14	-0.025 -0.242 -4.23 -11.44	0.0 -0.005 +0.019 -0.512 -2.55
	15	-0.027 -0.265 -4.23 -11.49	0.0 -0.096 -0.297 -1.47 -8.11
Speed	16	-0.014 -0.140 -2.12 -5.74	0.0 -0.044 -0.048 -0.691 -2.96
	17	-0.37 -0.359 -6.34 -17.23	0.0 -0.122 -0.133 -2.07 -8.87
	18	-0.047 -0.455 -8.45 -22.97	0.0 -0.154 -0.177 -2.77 -11.83
	19	-0.056 -0.545 -10.56 -28.70	0.0 -0.184 -0.221 -3.46 -14.79
	20	-0.064 -0.629 -12.67 -34.50	-0.212 -0.265 -4.15 -17.75
Body Shape	21	-0.024 -2.63 -4.23 -12.54	0.0 -0.088 -0.122 -1.28 -6.33

TABLE 4

LONGITUDINAL DENOMINATOR AND NUMERATOR ROOTS
WITH TRANSFER FUNCTION GAINS

	Gain	Roots			
Characteristic Equation		-0.0260	-0.2545	-4.2294	-11.486
N_δ^u	2.2754	-0.0277	-4.2558	-10.724	
N_δ^w	11.269	-0.0995	-0.2545	-7.6360	
N_δ^θ	17.067	-0.2545	-3.9964		
N_δ^z	11.269	-0.2546	-5.2091	+7.6985	

TABLE 5

LATERAL DENOMINATOR AND NUMERATOR ROOTS
WITH TRANSFER FUNCTION GAINS

	Gain	Roots			
Characteristic** Equation		-0.0864	-0.0886	-1.3823	-5.9142
N_δ^v	6.0237	-0.0886	-0.1839	-4.0579	
N_δ^ψ	7.0972	-0.0886	-1.003		
N_δ^ϕ	0.0	All roots zero due to no rudder control surface*			
N_δ^y	-6.0237	-0.0886	-1.4119	5.1244	

*When the base case data were modified to produce non-zero roll numerator coefficients it was found that the roll transfer function contained a free zero root in the denominator.

**A 5th root exists in the lateral CE with a value of zero which exactly cancels with a free zero in each lateral transfer function.

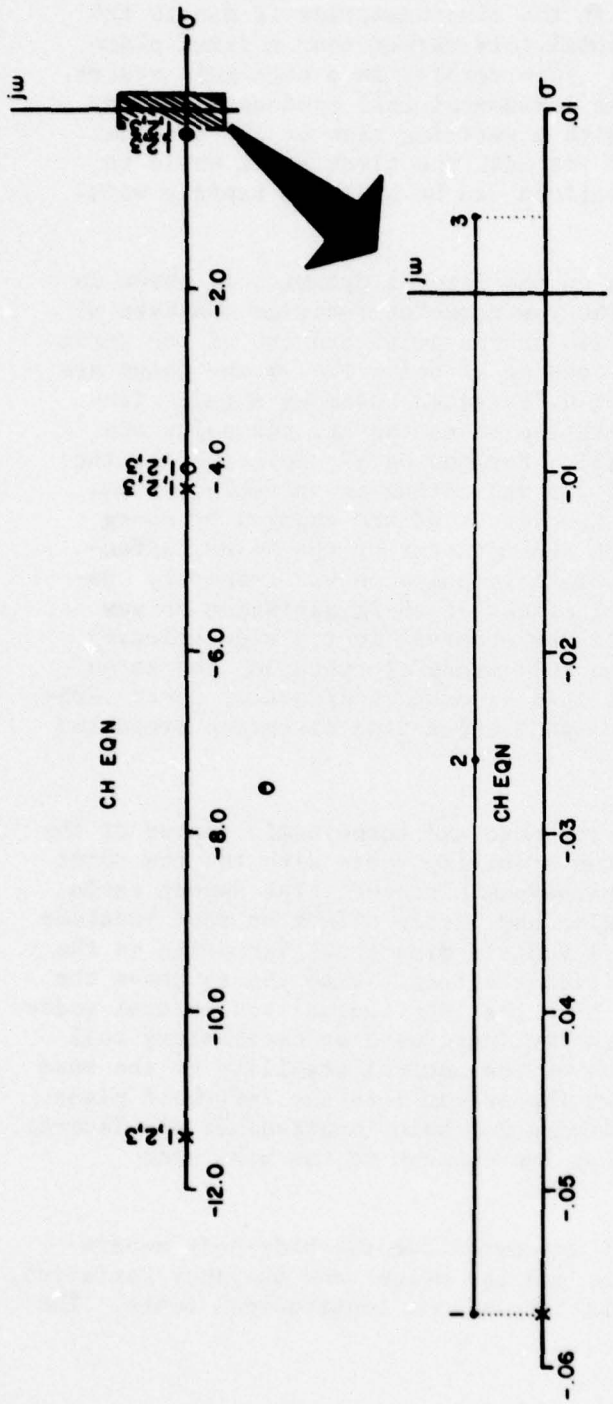

LONGITUDINAL

1 - cg 1/2" BELOW cb

2 - cg AT cb

3 - cg 1/2" ABOVE cb

FIGURE 4. ROOT LOCUS DIAGRAM OF VEHICLE PITCH FOR CB-CG VARIATION

inputs. The rapid response shown in the time histories is due to the selection of an all movable horizontal tail rather than a fixed plane with only a small portion movable. This results in a high gain system. For example, a 5-degree step in the horizontal tail produces a steady state pitch angle of 119 degrees with a settling time of 115 seconds. For this same input after only 5.8 seconds, the pitch angle would be 28.6 degrees. Thus, large pitch motions can be achieved rapidly with small tail deflections.

The effect of cb-cg variation on the lateral dynamics is shown in the yaw root locus of Figure 5. The yaw transfer function consists of three zeros and five poles. Only two of the poles and two of the zeros are affected by cb-cg change. For the cg ½" below the cb the poles are oscillatory with a damping ratio of 0.12 and an undamped natural frequency of 0.36 radians/second. With the cb at the cg, the poles are located at (s + 0.0) and (s + 0.089). For the cg ½" above the cb, the poles are at (s + 0.41) and (s - 0.32) indicating an unstable system. The two zeros of the yaw transfer function that are changed by cb-cg variation are seen to closely track the movement of the poles, effectively canceling the contribution of these poles on yaw response. Because of this cancellation, the net effect of cb-cg variation on yaw response is zero. This same result was observed in the side velocity transfer function. However for the roll transfer function, the zeros do not cancel the poles, and there is a pronounced effect of cb-cg variation on roll response as shown by the lateral time histories presented later in the report.

Varying the distance between the nose and aerodynamic center of the wing produced little movement of the stability roots with the tow point considered to remain at the wing aerodynamic center. The aspect ratio variation of the horizontal tail also had little effect on root location indicating little change in overall vehicle dynamics. Variation in the cb-cg did however, produce a significant effect. With the cg above the cb the vehicle became unstable in both the longitudinal and lateral modes. The low center of gravity configuration introduced an oscillatory roll mode in the lateral domain but removed the neutral stability of the base case by driving the lateral root at the origin into the left-half plane. Since this variation proved stabilizing for both longitudinal and lateral dynamics it definitely represents an improvement to the base case configuration.

Little variation in stability was noted for the body-body separation, the longitudinal cg position, and the weight and buoyancy variation, as noted by Table 3 which shows the lateral and longitudinal roots. The

(Text Continued on Page 14)

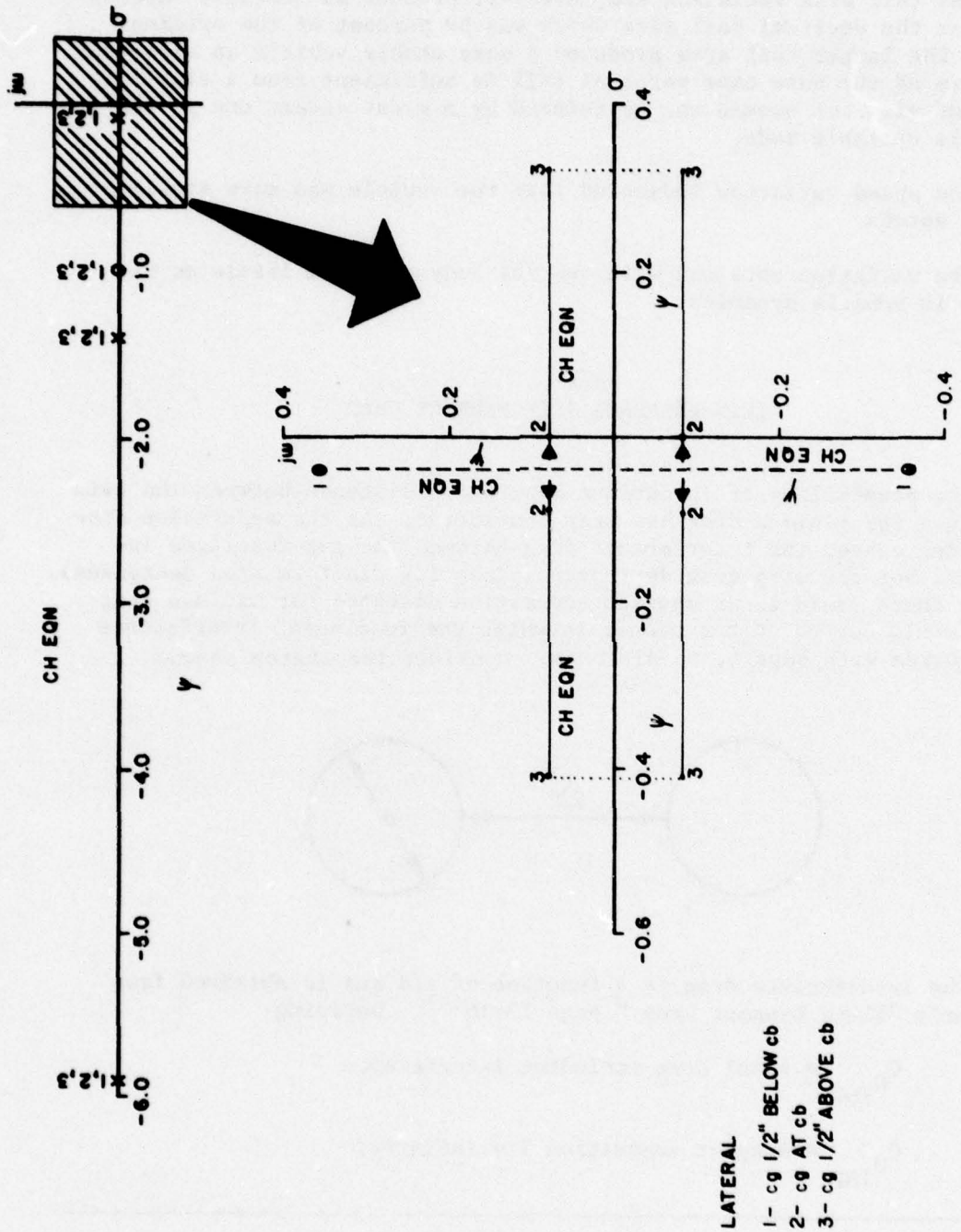

FIGURE 5. ROOT LOCUS DIAGRAM OF VEHICLE YAW FOR CB-CG VARIATION

vertical tail size variation did, however, produce an unstable lateral mode for the vertical tail size which was 50 percent of the original area. The larger tail area produced a more stable vehicle as expected. The size of the base case vertical tail is sufficient from a stability point of view but should not be reduced by a great extent due to the possible unstable mode.

The speed variation indicated that the vehicle was more stable at higher speeds.

The variation obtained with the 751 body produced little or no change in vehicle dynamics.

TWIN FUSELAGE INTERFERENCE DRAG

The possibility of an optimum separation distance between the twin fuselages for minimum drag has been considered. As the separation distance decreases, the interference drag between the two fuselages increases, but the wing drag decreases (since its planform area decreases). Hence, there could be an optimum separation distance for minimum drag which would depend on the manner in which the fuselages' interference drag varies with separation distance. Consider the sketch shown.

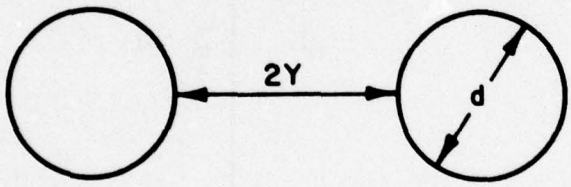

The interference drag is a function of Y/d and is obtained from Hoerner's "Fluid Dynamic Drag," page 13-16[4]. Defining

$C_{D_{TOT}}$ = total drag including interference

$C_{D_{INF}}$ = drag at separation Y = infinity,

---

[4]Hoerner, S. F., *Fluid Dynamic Drag*, Published by author, 1965.

the variation of $C_{D_{TOT}}/C_{D_{INF}}$ versus Y/d is shown in Figure 6. Obviously, the optimum separation distance will be at some value of Y/d less than 0.5. On the other hand, the present GTOPS configuration has a Y/d = 1.09. If the separation distance were reduced to Y/d less than 0.5, the loss of wing span (and planform area) would result in insufficient vehicle lift, unless outboard wings were added which would in turn increase the drag. Since the theoretical optimum design is not very practical, a separation distance was chosen which would yield a reasonable amount of wing lift rather than an optimum drag configuration.

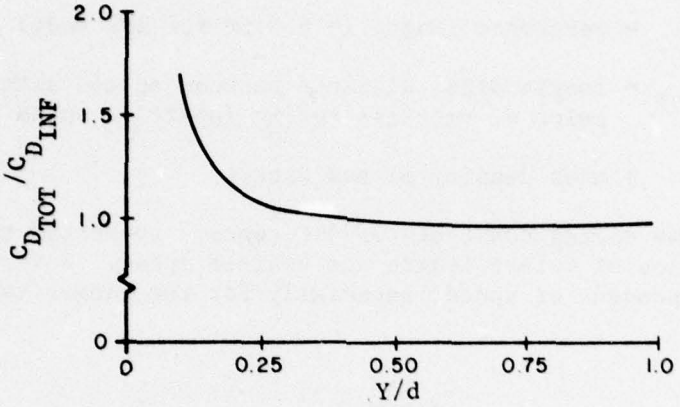

FIGURE 6. INTERFERENCE DRAG

EFFECT OF DEPTH-KEEPING TETHERS

ASSUMPTIONS

Reference 5 has been reviewed and appears to be correct within the limitations of the main assumptions: (1) neutrally buoyant tethers, (2) tangential cable drag negligible, and (3) main tow cable straight and vertical. Therefore, the computed effective vertical spring constants have been used in this analysis.

In this analysis, the depth-keeping tethers are modeled as a vertical spring of stiffness k attached to the vehicle. The effect of this vertical spring appears in the vehicle's equations of motion as the nondimensional hydrodynamic coefficients which follow:

---

(5) Applied Physics Laboratory, The Johns Hopkins University Report DM-3591, *GTOPS Mechanical Development Progress Report and Program Documentation,* by W. A. Venzia, 20 June 1977.

$$Z'_z = \frac{-k}{\frac{1}{2}\rho U^2 \ell} \qquad Z'_\theta = Z'_z\,(X_{TP}/\ell)$$

$$M'_z = Z'_\theta \qquad M_\theta = Z'_z\,(X_{TP}/\ell)^2$$

where

U = vehicle speed

ℓ = reference length (= 6.0 ft for APL body)

X_{TP} = longitudinal distance between cg and attachment point of vertical spring (positive ahead of cg)

ρ = mass density of sea water.

Table 6 shows spring constants of Reference 3 converted to values of Z'_z as a function of tether length and vehicle speed. Note that Z'_z is essentially independent of speed, especially for the longer tether.

TABLE 6

SPRING CONSTANTS CONVERTED TO Z'_z VALUES

Tether Length (ft)	U (knots)	k (lbf 1 ft)	$Z'_z \times 10^3$
64.2	4	1.8	-1.884
64.2	8	6.4	-1.675
64.2	10	10.4	-1.742
96.3	4	0.95	-0.994
96.3	8	3.75	-0.981
96.3	10	5.6	-0.938

ANALYSIS

Spring at CG, No CG-GB Separation

Three cases were analyzed. The first considered the effect of varying the spring constant k for a vehicle with the spring attached at the cg with zero cb-cg separation. The vehicle speed was 4 knots and the spring constant values were 0.0, 0.4, 0.8, and 1.6 lbf/ft. An investigation of the roots indicated that a non-zero spring constant introduces an oscillatory longitudinal mode with a decreasing period as k increases.

Spring at CG, CG Below CB

The second case covered the effect of varying the spring constant k for a vehicle with the spring attached at the cg and the cg one-half inch below the cb. Again, the speed was 4 knots and k had the values 0.0, 0.4, 0.8, and 1.6 lbf/ft. The results indicated that again as k increases above zero, oscillatory motion was encountered in the same manner as above; however, the overall damping was increased due to the effect of cb-cg separation.

Variation in Tether Attachment Point Location

The third case analyzed the effect of tether attachment location. The parameters for this study were a speed of 4 knots, zero cb-cg separation, a k of 1.6 lbf/ft, and tether attachment point locations (X_{TP}) of 1.0, 0.5, 0.25, 0.0, -0.25, -0.5, and -1.0 feet. The resulting roots (Table 7) indicate that the vehicle becomes unstable if the tether attachment point is behind the cg (negative values of X_{TP}). Figure 7 shows the effect of the longitudinal location of the tethers (X_{TP}) on stability. The pitch transfer function has five poles and three zeros; note that an additional pole and zero are present due to the tethers. Only two of the poles and zeros are affected by X_{TP} variation. For $0 \leq X_{TP} \leq 1.0$, the system exhibits lightly damped characteristics which means the system will have faster response and more overshoot than the system without tethers due to the spring effect of the tethers. For example at $X_{TP} = 0.5$, the poles are at $-0.019 \pm j\ 0.12$ and the zero is at -0.0166. The two poles are the characteristic mode of the system since they are closer to the origin than all other system poles. The damping ratio for these poles is 0.16. Because the zero is closer to the origin than the poles, the system will exhibit lead characteristics. For $-1.0 \leq X_{TP} < 0$, i.e. the attachment point behind the cg, the system is unstable, as witnessed by the single pole in the right-half plane.

(Text Continued on Page 19)

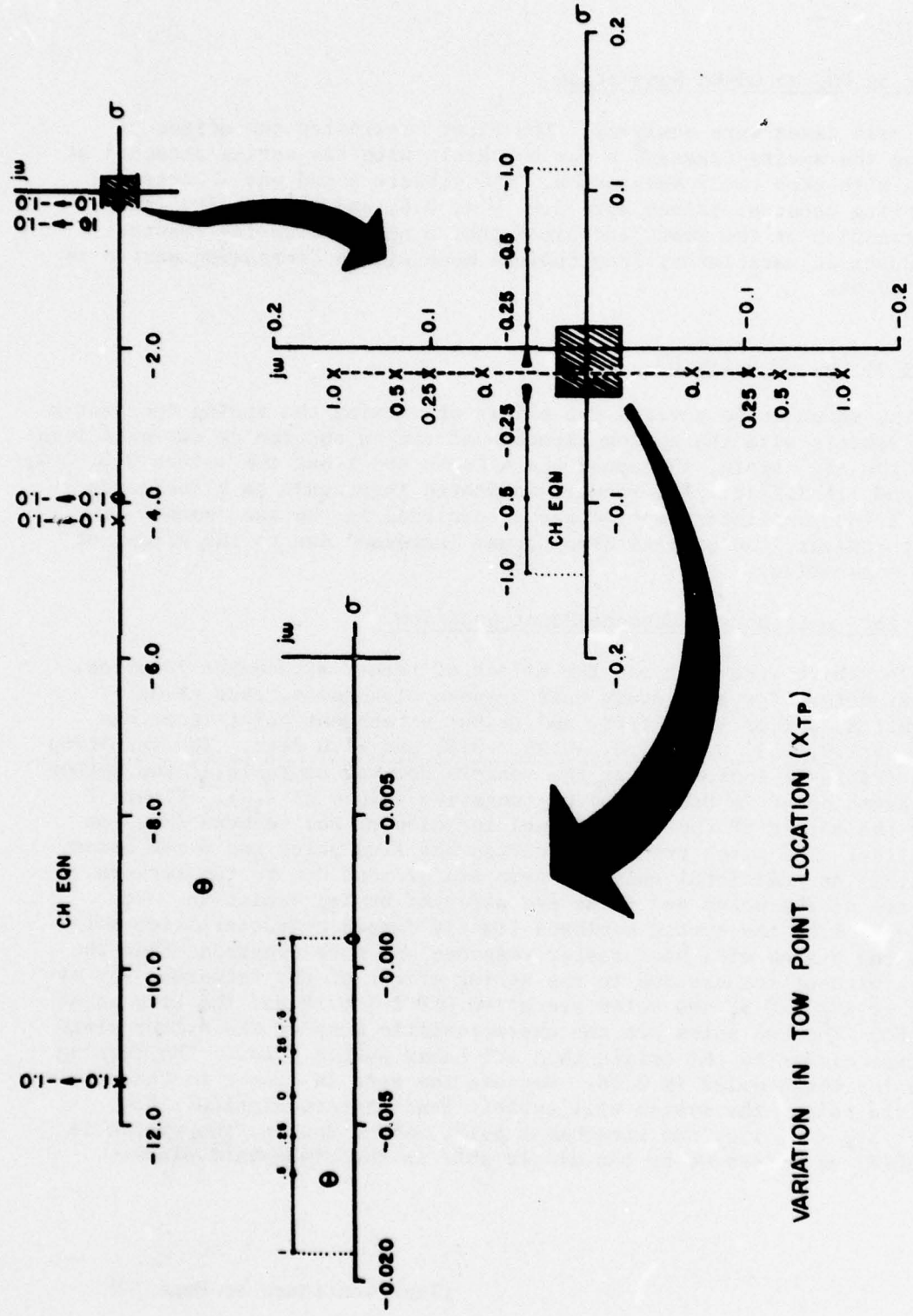

FIGURE 7. ROOT LOCUS DIAGRAM OF VEHICLE PITCH FOR TETHER ATTACHMENT POINT VARIATION

TABLE 7

LONGITUDINAL ROOTS FOR VARIOUS TETHER ATTACHMENT POINT LOCATIONS

X_{TP}	Longitudinal Denominator Roots				
1.0	-0.2546	-4.2152	-11.486	(-0.020 ± j 0.1587)	
0.5	-0.2546	-4.2169	-11.486	(-0.019 ± j 0.1213)	
0.25	-0.2546	-4.2177	-11.486	(-0.019 ± j 0.0973)	
0.0	-0.2546	-4.2185	-11.485	(-0.0188 ± j 0.0650)	
-0.25	-0.2546	-4.2190	-11.484	-0.0506	+0.0131
-0.5	-0.2546	-4.2200	-11.484	-0.0976	+0.0607
-1.0	-0.2546	-4.2220	-11.485	-0.1468	+0.1121

HORIZONTAL TAIL ACTUATOR

The torque required by the horizontal tail actuator is dependent upon the airfoil characteristics and the position of the stock. Positioning the stock as close as possible to the center of pressure will minimize the hinge moment due to the normal force acting at the center of pressure. However, should the center of pressure move behind the stock a reversal in the hinge moment will occur. Depending on the holding torque characteristics of the actuator, this phenomenon can cause the control surface to rotate to an uninitiated extreme deflection angle. The stock location is generally placed somewhat aft of the predicted locus of the center of pressure to avoid this problem. For this design the location of the center of pressure is expected to vary between 20 and 23 percent of the chord length for nonstall angles of attack ($|\alpha| \leq 25$ degrees). A stock position at the 25 percent chord yields hinge torques required to balance the moment due to the normal force of between 1600 and 1800 inch-ounces for $\alpha = 10$ degrees and a speed of 12 knots. At 4 knots this reduces to between 180 and 200 inch-ounces. It should be recognized that an angle of attack of 10 degrees is quite moderate. Required hinge torques will go up somewhat less than directly proportional to the angle of attack.

An important consideration here is that the holding torque must be sufficient to keep the control surface at a desired angle or vehicle characteristics will be altered.

LONGITUDINAL TIME DOMAIN ANALYSIS

TEST CONFIGURATIONS

The effects of cb-cg separation and depth-keeping tethers on the vehicle's longitudinal dynamics were determined from time histories. These time histories were generated by exciting the longitudinal transfer functions of the various configurations with various elevator forcing functions. Samples of the elevator or stern plane forcing functions are presented in Figure 8. The longitudinal variables examined in this series of tests were axial velocity u, normal velocity w, pitch angle θ, and depth change z. The matrix of tests as characterized by tether stiffness, cb-cg separation, and elevator forcing function is shown in Table 8.

TABLE 8

LONGITUDINAL DYNAMICS TESTS

Test No.	Tether Stiffness (lbf/ft)	cb-cg Separation (in.)	Elevator Function
1	No Tether	0.0	5 deg, 1 sec Pulse
2	No Tether	0.0	5 deg, 5.8 sec Pulse
3	No Tether	0.0	5 deg, 0.5 sec Doublet
4	No Tether	0.5	5 deg, 1 sec Pulse
5	No Tether	0.5	5 deg, 5.8 sec Pulse
6	No Tether	0.5	5 deg, 0.5 sec Doublet
7	1.6	0.5	5 deg, 1 sec Pulse
8	1.6	0.5	5 deg, 5.8 sec Pulse
9	1.6	0.5	5 deg, 0.5 sec Doublet
10	15	0.0	5 deg, 1 sec Pulse
11	15	0.0	5 deg, 5.8 sec Pulse
12	15	0.0	5 deg, 0.5 sec Doublet
13	15	0.0	15 deg, 1 sec Pulse
14	15	0.0	15 deg, 5.8 sec Pulse
15	15	0.0	15 deg, 0.5 sec Doublet

RESULTS

Two points about the results need to be emphasized. First, the results given here are for a vehicle speed of 4 knots. The trends should be the same at other speeds, but the magnitudes; e.g., depth change, will not. Second, some cases involving pulses of 5.8 seconds duration are invalid because they involve vehicle motions (especially pitch) which exceed the small perturbation assumptions on which the linear analysis is based.

Without Tethers

Without tethers, the vehicle motion is essentially aperiodic, and any disturbance produces a finite, steady state depth change (Figure 9). However, cb-cg separation (cg below cb) increases the pitch stability and reduces the magnitude of this finite depth change (Figure 10). For example, the depth change caused by a 5 deg, 1 sec pulse is reduced from 54 feet to 28 feet when the cg is moved 1/2 inch below the cb.

With Tethers

With tethers, the vehicle motion is oscillatory (with the exception of u which remains aperiodic because the vertical spring does not couple into the axial motion) and the final, steady state depth change is zero. For a tether stiffness of 1.6 lbf/ft (Figure 11), the damped natural period is 101.5 second and the time to damp is 88 second (3 time constants), while for a tether stiffness of 15 lbf/ft (Figures 12 and 13), the damped natural period is 31.7 second and the time to damp is 44 second. It should be noted that the stiffness at 4 knots will probably be on the order of 1.6 lbf/ft and not 15 lbf/ft.

LATERAL TIME DOMAIN ANALYSIS

TEST CONFIGURATIONS

The effect of cb-cg separation on the vehicle's lateral dynamics was also determined from time histories. These time histories were generated by exciting the lateral transfer functions of the various configurations with various rudder forcing functions (see Figure 8). The lateral variables examined in this series of tests were sideslip velocity v, yaw angle ψ, roll angle ϕ, and side track y. The matrix of tests as characterized by cb-cg separation, rudder type, and rudder forcing function is given in Table 9. Please note that rudder type "No Lower" means that only the upper rudder is moveable; the vehicle still has symmetric upper and lower vertical stabilizers. This special case was run simply to provide a means of exciting the zero cb-cg separation configuration in roll.

(Text Continued on Page 28)

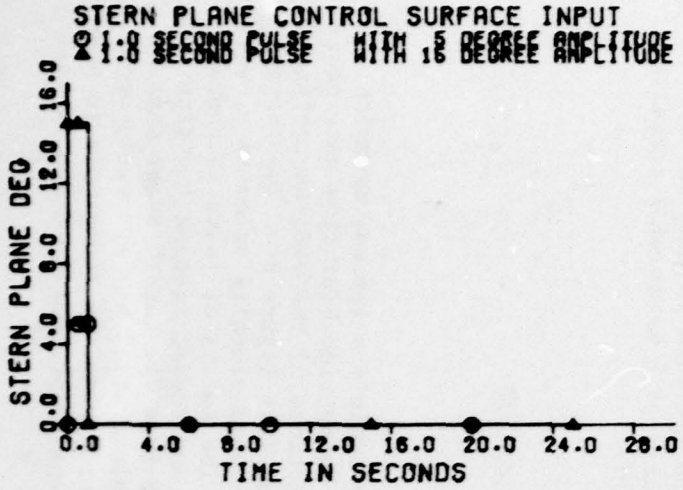

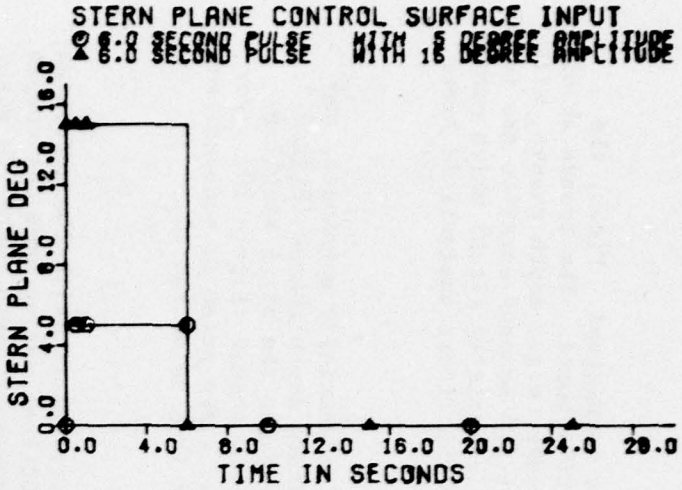

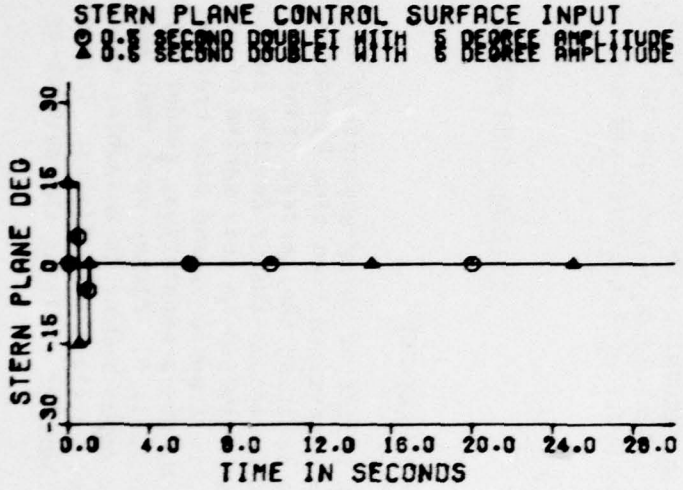

FIGURE 8. STERN PLANE FORCING FUNCTIONS FOR LONGITUDINAL RESPONSE

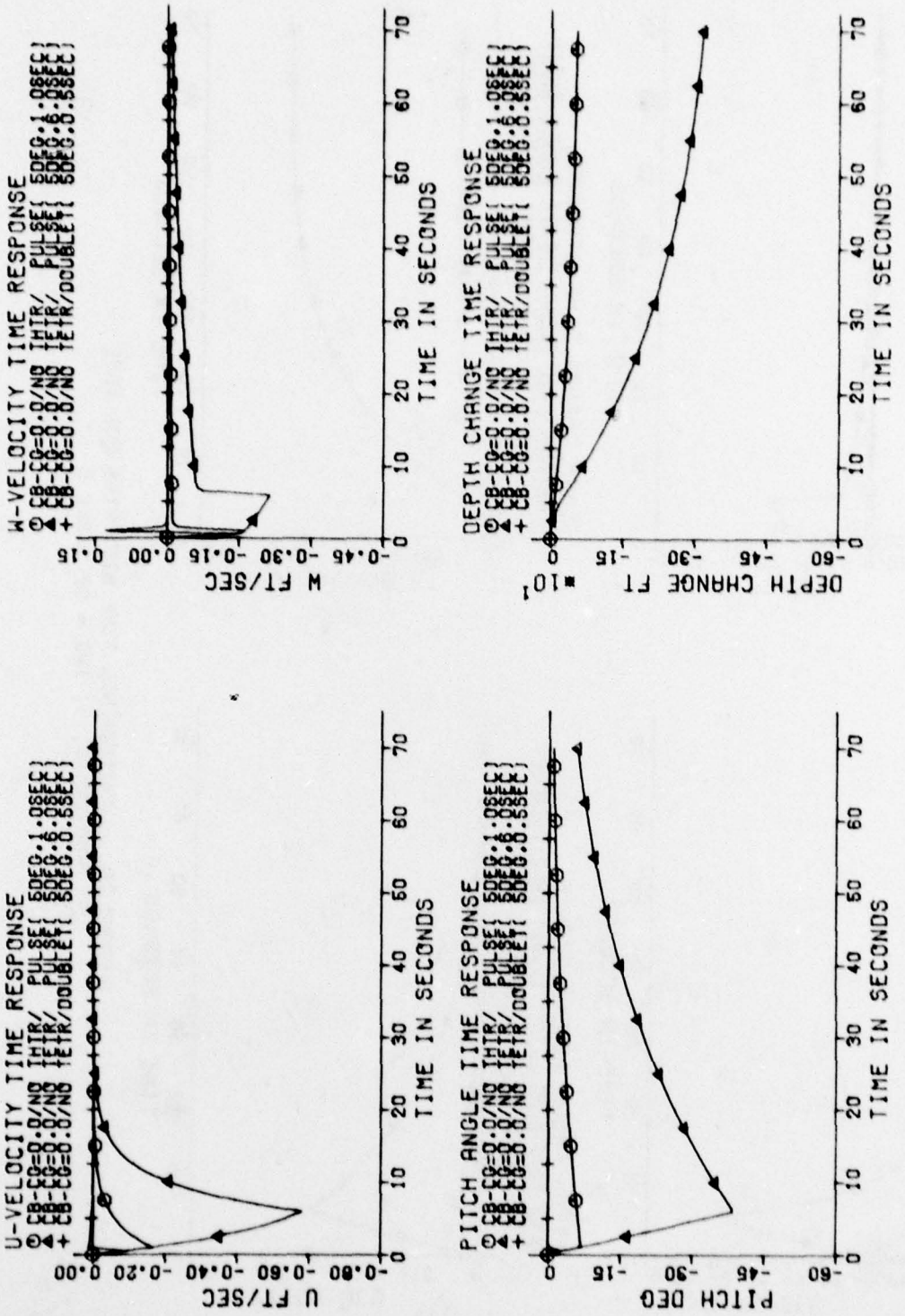

FIGURE 9. LONGITUDINAL TIME HISTORIES FOR TEST NUMBERS 1, 2, AND 3 OF TABLE 8

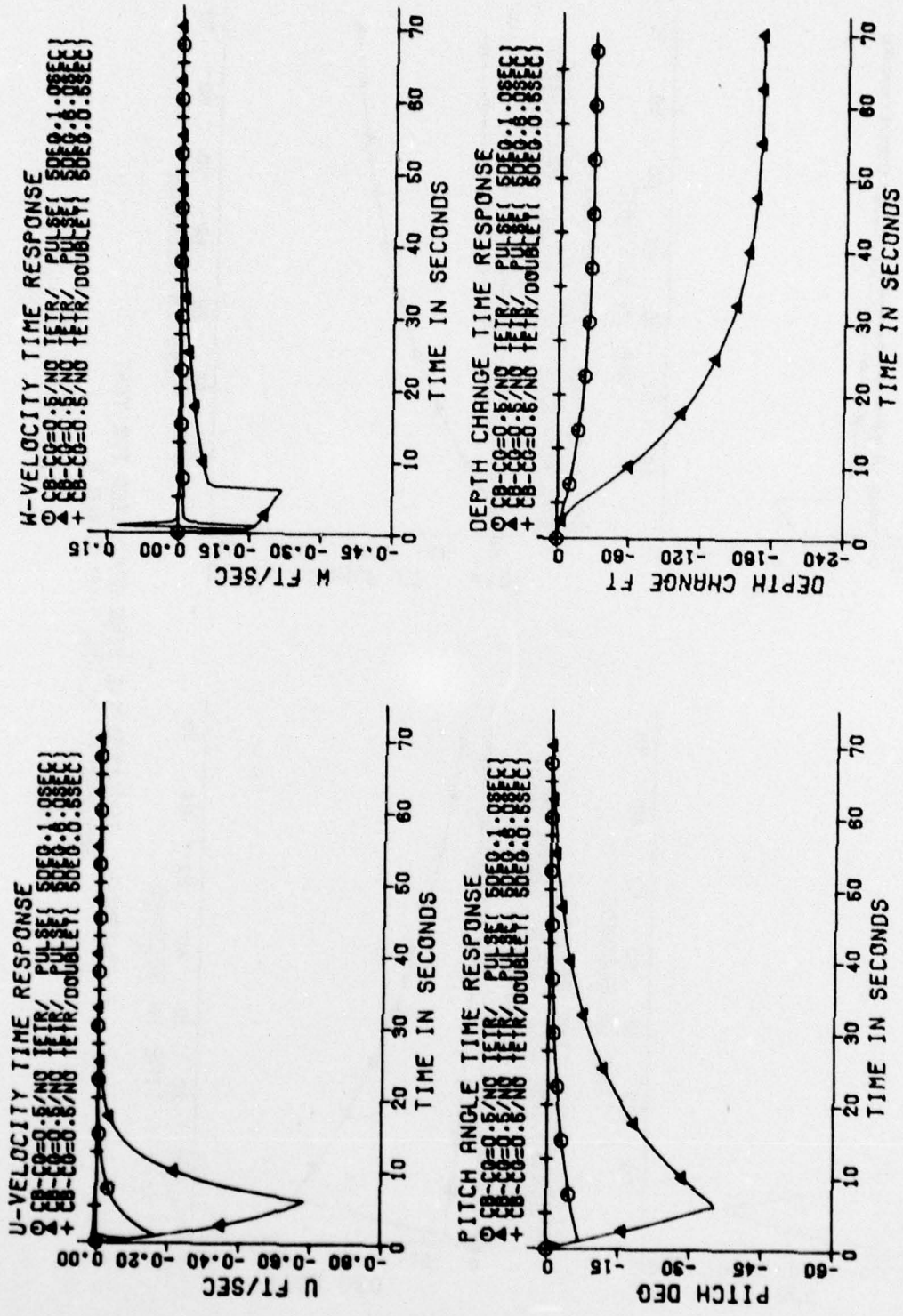

FIGURE 10. LONGITUDINAL TIME HISTORIES FOR TEST NUMBERS 4, 5, AND 6 OF TABLE 8

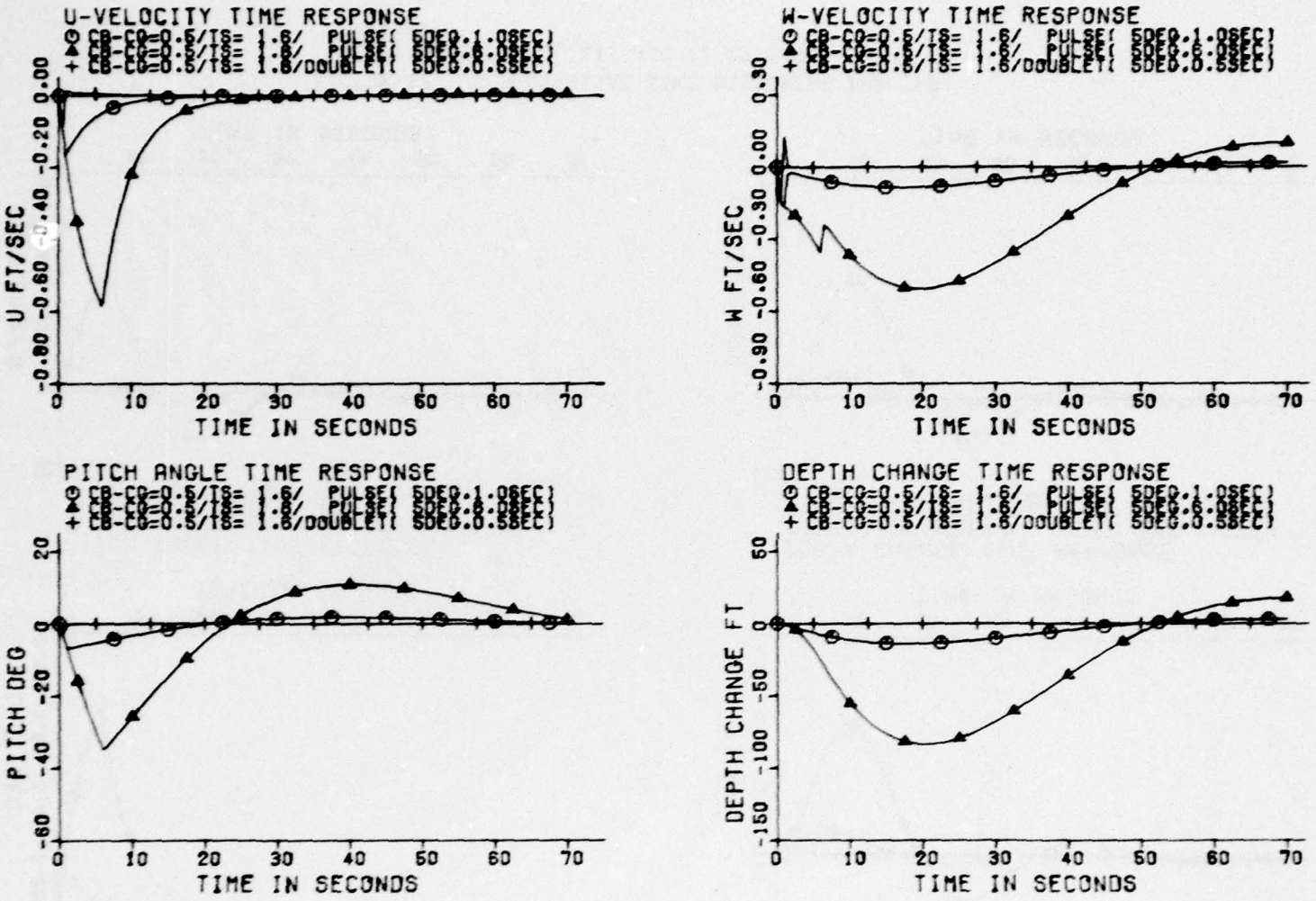

FIGURE 11. LONGITUDINAL TIME HISTORIES FOR TEST NUMBERS 7, 8, AND 9 OF TABLE 8

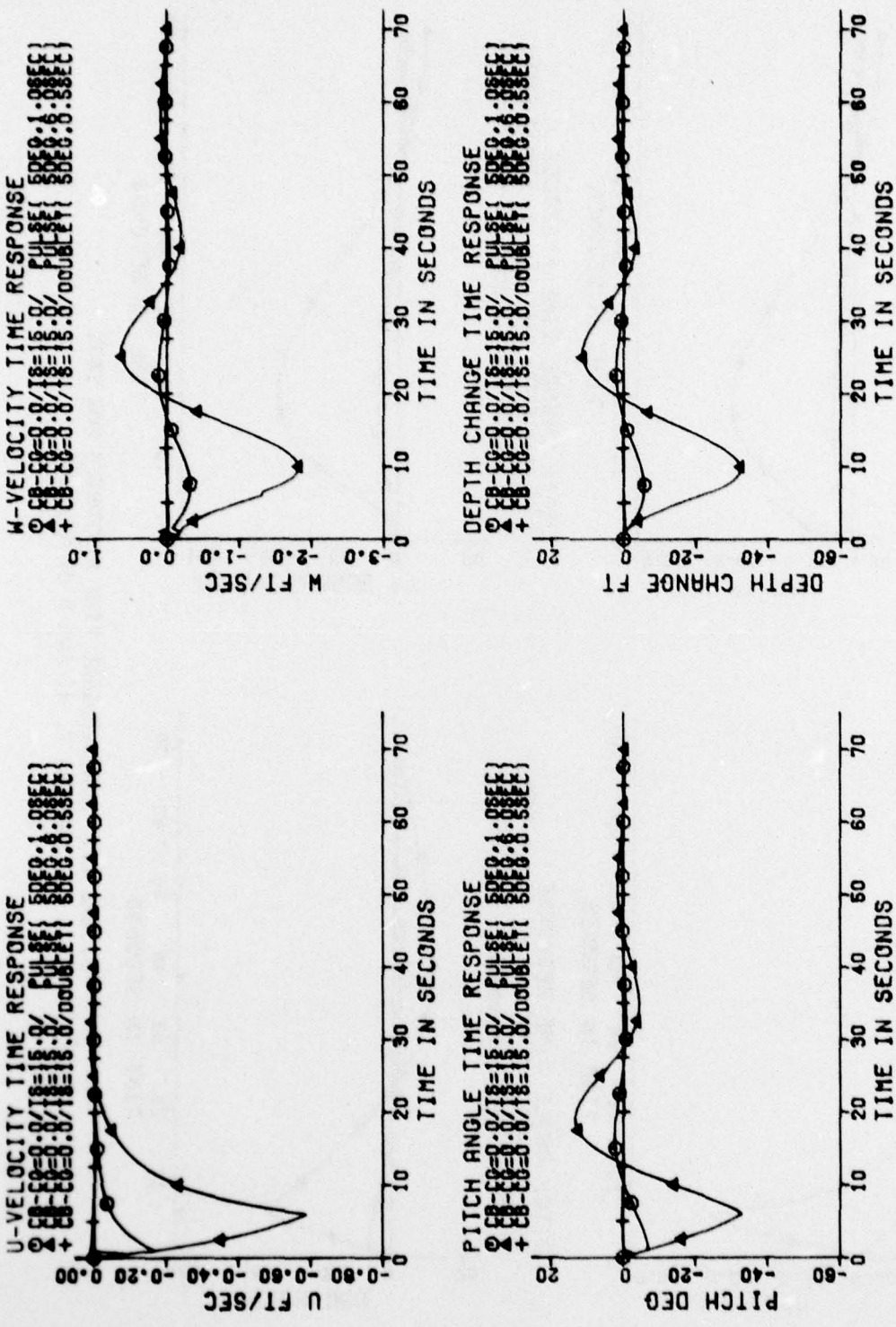

FIGURE 12. LONGITUDINAL TIME HISTORIES FOR TEST NUMBERS 10, 11, AND 12 OF TABLE 8

FIGURE 13. LONGITUDINAL TIME HISTORIES FOR TEST NUMBERS 13, 14, AND 15 OF TABLE 8

TABLE 9

LATERAL DYNAMIC TESTS

Test No.	cb-cb Separation (in.)	Rudder Type	Rudder Function
1	0.0	No Lower	5 deg, 1 sec Pulse
2	0.0	No Lower	5 deg, 0.5 sec Doublet
3	0.0	Symmetric	5 deg, 1 sec Pulse
4	0.0	Symmetric	5 deg, 0.5 sec Doublet
5	0.5	Symmetric	5 deg, 1 sec Pulse
6	0.5	Symmetric	5 deg, 0.5 sec Doublet

RESULTS

As noted in the longitudinal analysis, the results given here are for 4 knots. The trends should be the same at other speeds, but the magnitudes; e.g., side track, will not.

This analysis assumes that neither the tow cable nor the depth-keeping tethers produce roll moments or side forces. In the actual vehicle, they will be coupled with both roll and side track, but determination of these coupling terms would require a more sophisticated analysis. The present analysis, however, has demonstrated the need to have both roll and side track restoring moments and forces present in adequate amounts. The time history plots described in Table 9 are presented in Figures 14 through 16.

No cb-cg Separation

Without cb-cg separation, the vehicle motion is essentially aperiodic and any disturbance will produce finite, steady state values of side track and roll (Figure 14). For example, a 5 degree, 1 second pulse of only the upper rudder causes a final roll angle of 16 degrees and a final side track of 2.4 feet.

(Text Continued on Page 32)

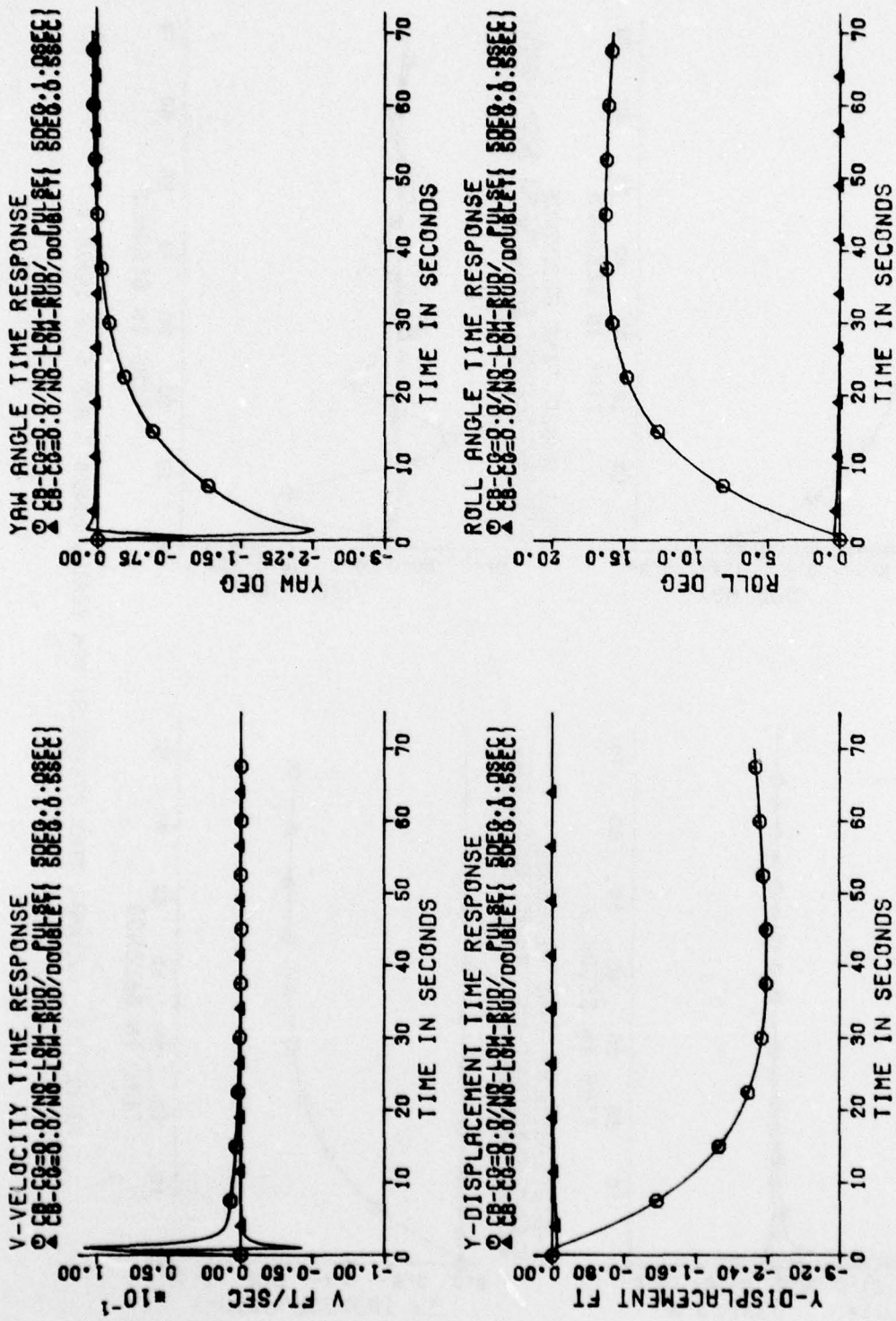

FIGURE 14. LATERAL TIME HISTORIES FOR TEST NUMBERS 1 AND 2 OF TABLE 9

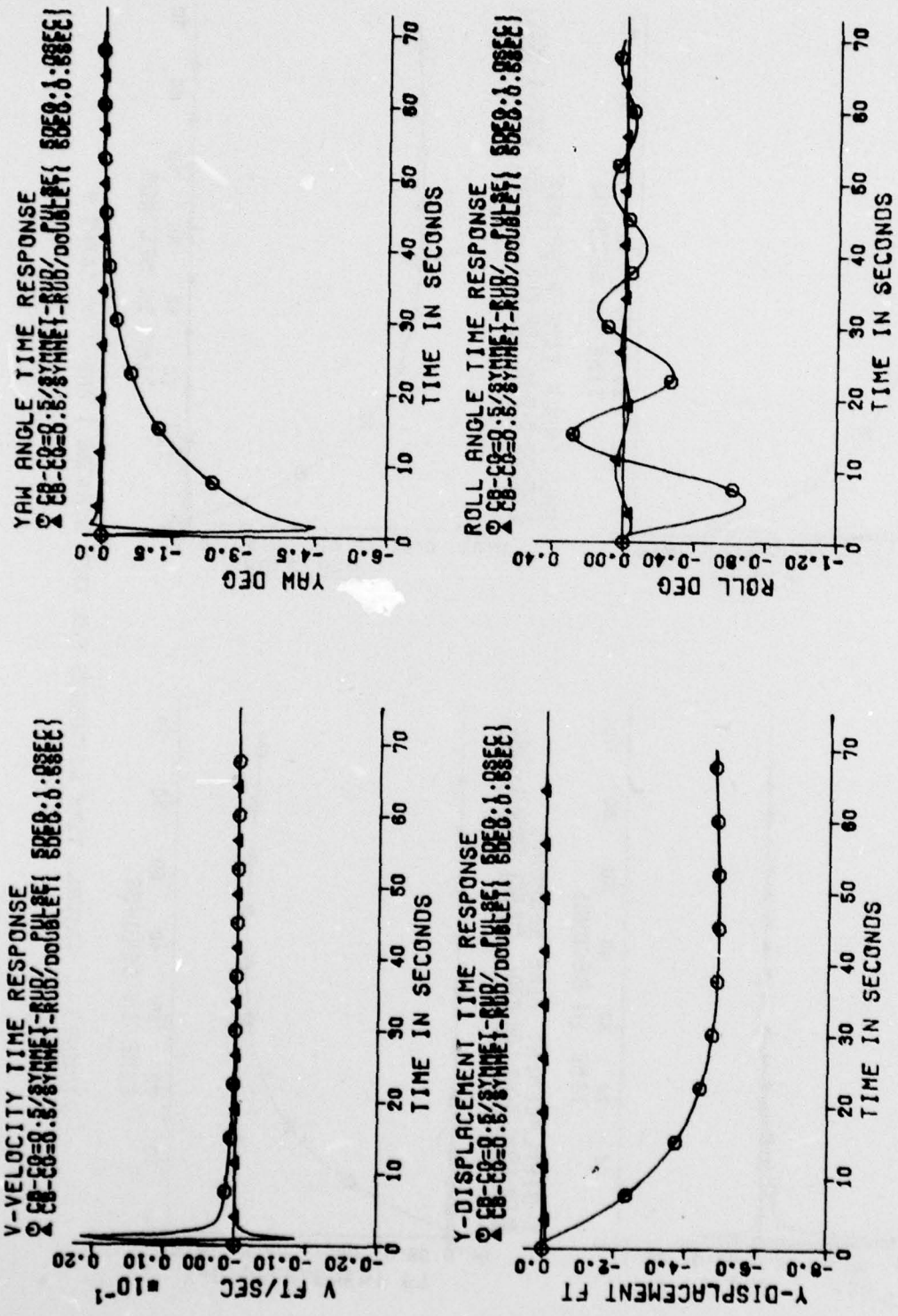

FIGURE 15. LATERAL TIME HISTORIES FOR TEST NUMBERS 3 SNF 4 OF TABLE 9

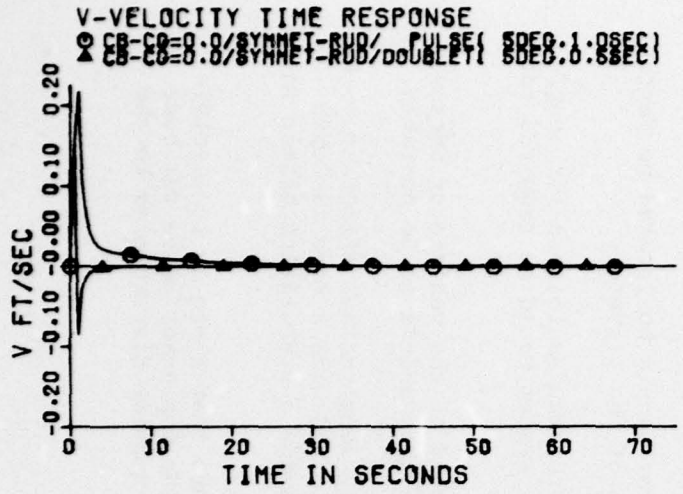

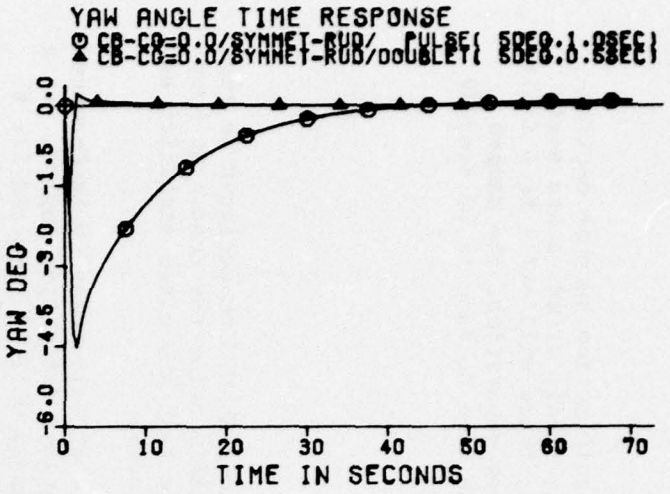

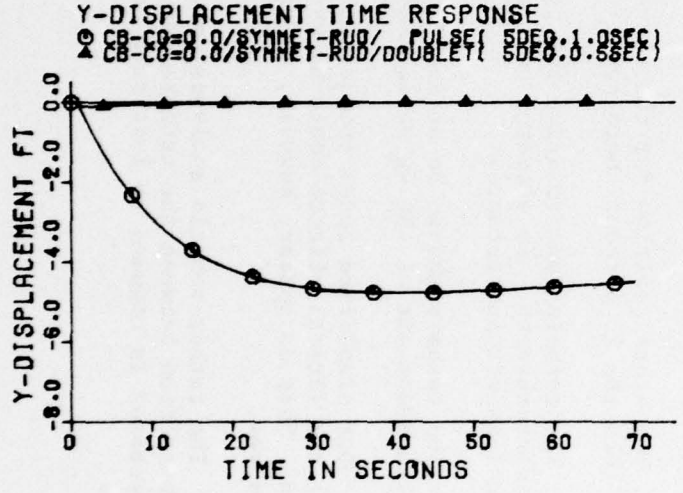

FIGURE 16. LATERAL TIME HISTORIES FOR TEST NUMBERS 5 AND 6 OF TABLE 9

With cb-cg Separation

With cb-cg separation, the vehicle's roll motion becomes oscillatory (v, ψ, and y remain aperiodic) and the final, steady state angle will be zero (Figures 15 and 16). However, there will still be a finite, steady state side track. For 1/2-inch cb-cg separation, the damped natural roll period is 17.4 seconds and the time to damp is 68 seconds (3 time constants).

CONCLUSIONS

1. The mass distribution of the vehicle should be designed so that the center of gravity is positioned vertically below the center of buoyancy as far as possible. This will provide roll and pitch stability as well as minimum depth loss due to disturbances.

2. A horizontal tail actuator capable of delivering 50 inch-ounces of torque is insufficient for moderate elevator deflection angles. At a speed of 4 knots approximately 100 inch-ounces will be required for a deflection angle of 5 degrees (this is for the tethered vehicle with 1/2 in. cb-cg separation). An actuator slop of 1/4 of a degree for the elevator will result in an error of 1 degree in pitch and 8 feet in depth at 4 knots.

3. The stock position for the elevator should be located no further forward than the 25 percent chord position of the elevator.

4. The tethers tend to drive the depth changes to zero for longitudinal disturbances. An elevator control system would be required for no depth loss without tethers.

5. The tethers should be attached ahead of the vehicle cg because their attachment aft of the cg would cause the vehicle to be unstable.

6. Our simplified model predicts only longitudinal effects for the tethers; the lateral effects could be estimated with a more in-depth analysis. They do appear, however, to provide a stabilizing effect in roll and yaw.

7. The tether-vehicle analysis assumes that there is no significant interaction between the tethers and the depressor below the body (the depressor is assumed to institute no dynamic disturbances to the system).

8. Based on the tether analysis provided to NCSL[5], a 1.6 pound/foot spring constant is a reasonable estimate at 4 knots. The frequency of oscillation predicted by this analysis is, however, too high by a factor of the square root of 32.17. The analysis presented in this report for a spring constant of 1.6 calculated a longitudinal oscillatory period of 101.5 seconds. This period is much higher than that predicted by the analysis treating the body as a spring mass system assuming no pitch coupling. This difference implies that the coupling cannot be neglected. In general it is questionable whether or not a linear spring constant of 15 pound/foot can be achieved for the anticipated tethered vehicle design.

9. Although a vertical cb-cg separation does provide for roll stabilization, some consideration should be given to adding partial span ailerons to the wing of the body to provide adequate roll control.

10. Coupling of longitudinal and lateral motions are instituted by both hydrodynamic and tether forces. A nonlinear analysis would require the knowledge of nonlinear hydrodynamic and coupling coefficients. The linear analysis provided here assumes no coupling. A nonlinear analysis would require a much more detailed investigation. Past experience with other towed vehicles has indicated that as long as vehicle motions about an equilibrium state are "small" the linear equations have been found to adequately describe its dynamics.

---

[5]ibid.